Journal of Electronic Imaging 1(2), 136-142 (April 1992).

Marker-controlled segmentation: an application to electrical borehole imaging

Jean-François Rivest
Serge Beucher
Ecole des Mines de Paris
Centre de Morphologie Mathématique
35, rue Saint-Honoré
77305 Fontainebleau, France

Jean-Pierre Delhomme
Etudes et Productions Schlumberger
26, rue de la Cavée
P.O. Box 202
92142 Clamart Cedex, France

Abstract. *An application of marker-controlled segmentation in petroleum engineering is presented. The images to be segmented originate from high-resolution conductivity measurements of borehole walls. These measurements reflect the composition and structure of the rock formation through which the well was drilled. In this application, we detect and measure small cavities, or* vugs, *in the walls. We use the tools provided by mathematical morphology. Our strategy is based on gradient image modification using markers and on the watershed transformation. First, the vugs are automatically marked, as well as the background. These markers together delineate areas of interest in which we know there is one contour per vug. To find the vug contour and perform measurements, we modify the gradient image in such a way that only a single edge is kept between the vug and the background markers. We perform the final step of edge detection using the watershed transformation of the modified gradient image. The final result is one closed contour per marked vug. This strategy is presented in detail, experimental results are shown, and artifact elimination is discussed.*

1 Introduction

Two basic approaches to image segmentation exist. The first one is boundary-based and detects local changes. The second is region-based and searches for pixel and regional similarities.[1,2] They both attempt to degrade image data as gracefully as possible to extract tokens to be passed to higher level analyzers.

The most widely used set of tokens is the edge map: Objects in images are represented by their edges, giving a caricature-like representation of them. There are good reasons to adopt this type of image representation. From a computational point of view, an edge map neatly represents image data: It is compact and we may devise powerful algorithms to extract from it characteristics such as length, curvature, and so on. This representation is also consistent with experimental results from physiology, which tend to confirm the existence of such mechanisms in vision processes.[3]

In the application that we present here, the cartoon-like approach proposed by Marr and Hildreth[3,4] is inoperative because it experiences two implementation problems. The first of these problems originates from the implementation of the edge finder. It is not a trivial task and most of the approaches used to achieve this goal require the parameters to be carefully adjusted for a specific application. An example of an edge finder is the thresholding of gradient images.[5] This is sensitive to noise and threshold parameters and gives thick and incomplete edges. A more sophisticated algorithm uses heuristic search.[6,7] It consists roughly of two major stages: First, the algorithm selects a starting point on a contour. Then, it attempts to search the best neighboring pixel continuing the contour. The criterion is a cost function and is defined using heuristics. It also needs a criterion in order to know when to stop. It gives better results, but we have to define heuristics, cost functions, and the start and stop criteria with care. These heuristics vary from one application to another and may be difficult to find. Edge finding using zero-crossings of the second derivative of images is sensitive to noise and quantification errors. Blurring filters may be used to improve the SNR and regularize the ill-posed problem of derivation,[8] but their action is antagonistic toward edge detection. Moreover, the use of these filters implies an *a priori* knowledge of object size. In our application, this knowledge is not available.

To provide an answer to the problem of finding edges in images, Beucher and Lantuéjoul[9] proposed the use of the watershed transformation on gradient images. The definition of this algorithm comes from an analogy with topography; pixel intensities are considered as altitudes. On a relief,

Paper 91-008 received May 14, 1991; revised manuscript received Feb. 13, 1992; accepted for publication Feb. 21, 1992.
1017-9909/92/$2.00 ©1992 SPIE and IS&T.

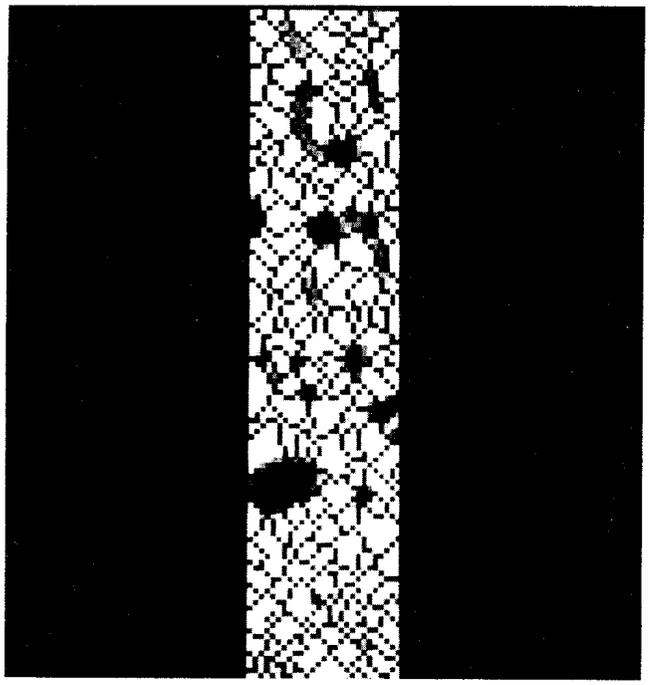

Fig. 1 The watershed transformation of gradient images leads to oversegmentation as seen on this edge map superposed over the input image. Most of the segmentation methods have this problem in common.

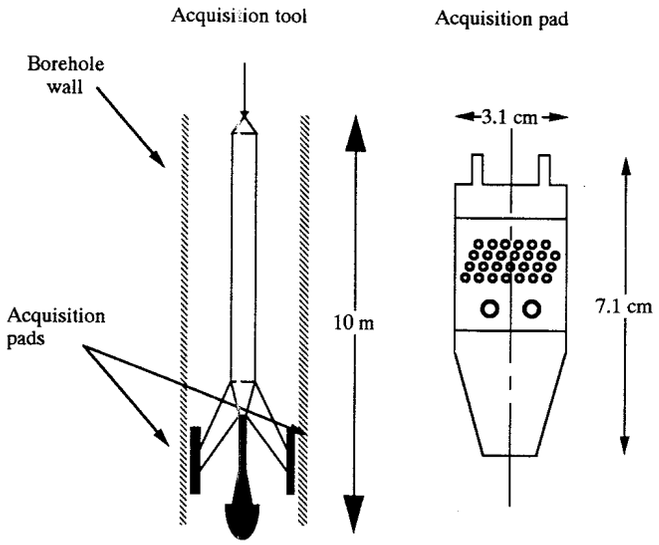

Fig. 2 Acquisition tool principle. On the left, the tool scans the walls of a well. On the right is a schematic close-up of one pad. Circles represent electrodes. (Not to scale.)

there are minima or lake draining areas called *catchment basins*. The boundaries between these areas are watersheds. The watershed transformation finds crestlines on images by growing catchment basins out of minima, which is a lot easier than finding these lines directly. We give a precise definition of this transformation later in this paper. It is a powerful approach, but it experiences difficulties that are not much different from the second problem of Marr's caricature-like representation: There are too many edges and we must find a strategy to eliminate them. Figure 1 shows this oversegmentation problem in a borehole image.

A strategy has been proposed by Meyer and Beucher[10,11] to overcome this problem. This strategy is called *marker-controlled segmentation* and has successfully been applied on electrophoresis gel characterization,[10,12] road detection,[13] and cardiology.[14] The main idea underlying this approach is that often machine vision systems "know" roughly from other sources the location of the objects to be segmented.

This approach is applied as follows: We generate a marker for each of the objects to be segmented. We do the same for the background, i.e, for portions of the image where we are sure no pixel belongs to any object. The remainder of the procedure is straightforward and is the same for all applications: We modify the gradient image in order to keep only the most significant contours in the areas between the markers. Then, on the modified gradient image we perform a final contour search using the watershed transformation. No supervision, no parameter, and no heuristic is needed to perform the final segmentation. The parameters controlling the segmentation are concentrated in the marker construction step, which is the easiest place to control and validate them. The markers may be generated either manually or automatically. This is an important aspect of the method: Markers may be determined by means of different sources. For instance, user input, specialized sensors, and feature detectors can be used. The search of the final contour is automatic and has no parameter. It is independent of the application.

We used this approach for a specific application from the oil industry. Sections 2, 3, and 4 describe the application, while Sec. 5 presents the results we obtained from our approach. We provide details on the application that may seem superfluous in a vision paper. However, these details illustrate how we approached the problem, and may show how a generalization can be done for other vision tasks.

2 Acquisition

The images were obtained from a Formation MicroScanner,™ a tool used in the oil industry to scan borehole walls for examination of the underlying geological structures.[15] It works by injecting high-frequency currents into the formation through an array of electrodes scanning the walls. These electrodes are located on pads pressed against borehole walls by hydraulic devices, as shown in Fig. 2. Current intensities are acquired, measuring geological formation conductivities. Images are generated by the moving array of electrodes. Pixel gray levels are a representation of the rock formation conductivity, and the whole acquisition process has to be modeled in order to make quantitative measurements of the images. It is an unusual vision problem: We had to use knowledge about the tool response instead of the usual assumptions made for scene analysis, which are related to the eye/brain response.

The images are an internal unwrapped view of the borehole walls, the horizontal axis being the angle θ in a cylindrical coordinates system, while the vertical axis is associated with depth. Due to the limited pad width, we do not have a complete view of the wall. Instead we have strips corresponding to the acquisition pads. The strip width is 27

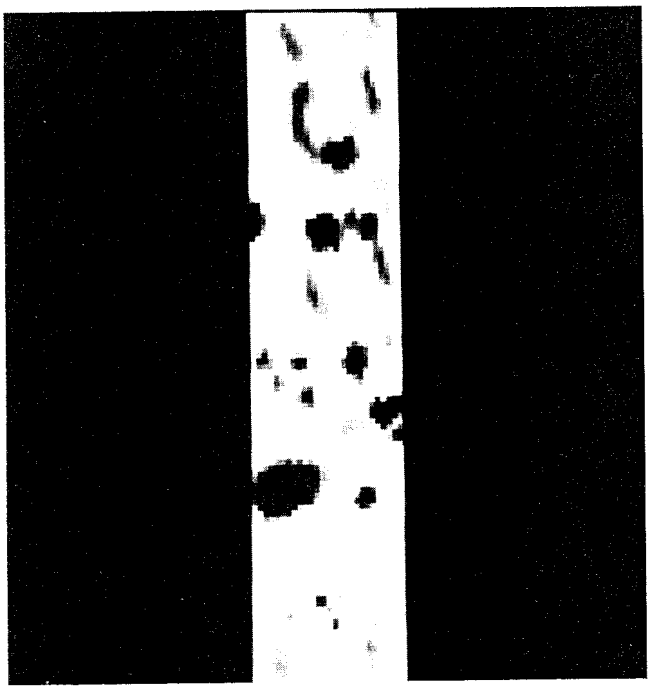

Fig. 3 Original input image. Dark areas represent high conductivity values. Original height is about 30 cm.

pixels, each pixel representing a square of 2.5×2.5 mm. Figure 3 shows a typical image obtained with this tool.

The application is devoted to vug detection in these images. Vugs are small cavities in the rocks and can be compared with pores in a sponge, allowing oil and gas to be stored in the formation. During the drilling process, these vugs are filled with conductive mud giving local conductivity maxima in the images. Numerical modeling of the tool response has shown that a vug boundary corresponds to an inflexion line, which may be detected using gradient maxima. The inflexion line is seen as a crest line in gradient modulus images. Further modeling results showed that there is a relationship between conductivity contrast, detected size, and vug depth. These results enabled us to qualify the vugs we detected in terms of depth. It was also useful for artifact elimination, as we show in Sec. 4. Figure 4 shows a typical image profile.

3 Processing

From these criteria, we have to find robust detectors. We describe in this section how we constructed them. We then detail the algorithms.

3.1 *Preprocessing*

We improve the SNR of images by using morphological filtering. Vugs are maxima in images. We need to preserve these maxima, but we also need to merge them when they are separated by only a few pixels.

Dilation can perform maxima merging. It is implemented most of the time like median filters, except that the operator outputs the maximum over a given neighborhood, instead of the median value. The shape of the neighborhood is determined by a *structuring element*. The problem is that

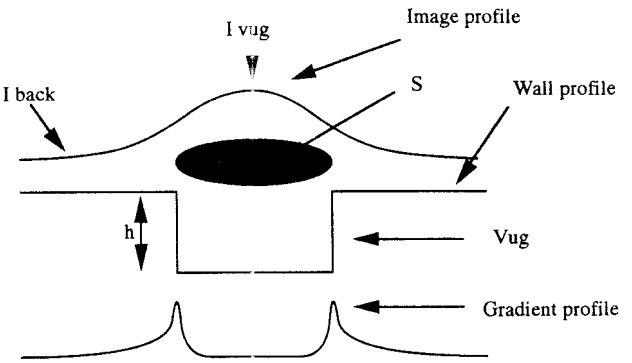

Fig. 4 Typical image profile caused by a vug. Top: image profile, middle: underlying vug, bottom: gradient profile, where S is the surface of the actual vug. It is used to determine rock porosity after the segmentation is performed.

the dilation operator enlarges the maxima. If the maxima do not merge, these must be shrunk back to their original size. This is achieved by eroding the dilated image. Erosions are dual operators with respect to dilation: The operator takes the minimum over the neighborhood instead of the maximum as in the dilation. The cascade of a dilation $\delta(f)$ followed by an erosion $\varepsilon(f)$ is called a *morphological closing*, denoted $\phi(f)$, where f is the input image and *fil* is the filtered image:

$$fil = \phi(f) = \varepsilon[\delta(f)] \ . \tag{1}$$

In this application, we use a morphological closing with a diamond-shaped structuring element of size 1.

In the approach, the preprocessing steps may vary. For example, we could have used linear filters instead of the closing filter. In our application, morphological closing performed the best in merging maxima separated by an interval smaller than the diameter of the structuring element. However, no general procedure yet exists to find good filters.

3.2 *Marker Image Generation*

Markers play a central role in the approach we present here. This section describes the algorithms we used to get them.

Object markers

As we mentioned in Sec. 2, a vug is a local maximum in conductivity images. The choice among object markers is not critical, if they fulfill the following requirements:

1. Each object must have a unique marker; more than one marker will lead to oversegmentation.
2. The marker must be located inside the object.

Mathematical morphology provides an excellent maxima detector.[10] A maximum is a region of pixels where there is no descending path going to it. The detector is implemented as follows:

$$Om = fil - \text{recons}(fil, fil - 1) \ , \tag{2}$$

where *fil* is the preprocessed image $\phi(f)$, *Om* is the object marker function, and recons(*marker*,*constraint*) is the mor-

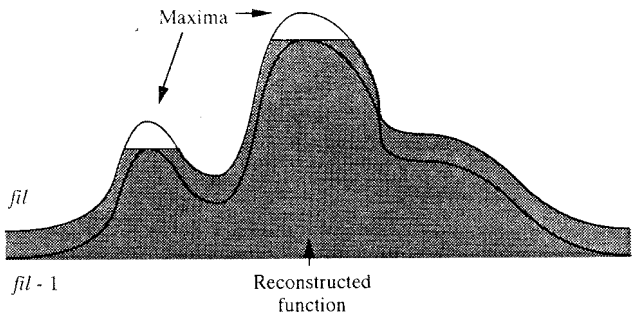

Fig. 5 Morphological maxima detector. The maxima of *fil* − 1 are propagated on the image plane (horizontally) until stability. The maxima are then found by comparison with the original image *fil*.

phological function reconstruction operator. This operator is implemented in the following manner for the digital case.

recons(*marker*,*constraint*) =

Repeat:

$$marker_{n+1} = \min[\delta_B(marker_n), constraint]$$

until $marker_{n+1} = marker_n$, (3)

where $\delta_B(marker)$ is the dilation of the marker function *marker* by the planar structuring element B, the digital disk of diameter 1. The result of each iteration is put back into *marker;* that is, we first dilate *marker*, then prevent it from getting over *constraint* by taking the minimum between these images. The image obtained is then dilated and the iteration is executed again until the resulting image is stable. Figure 5 illustrates how the maxima detector works.

Background markers

The outside of a vug is located at conductivity minima. However, it is preferable to define the background of a vug in terms of paths joining these minima. These paths should minimize the average intensity. They should pass at the bottom of intensity "valleys" in the image.

Again, the choice among many detectors is not critical, provided the following requirements are met:

1. Object and background marker must not touch each other; the final contour would not be able to pass between them.
2. The background marker delimits an area of interest in which the object resides. It therefore has to be outside the object.

We used the watershed of the complement or inverse of the filtered image *fil* to create the background marker *Bm*:

$$Bm = \text{watershed}(-fil) \quad (4)$$

The watershed transformation comes from an analogy of image data with the surface of a landscape, as shown in Beucher[10] and Soille and Ansoult.[16] This landscape has peaks, valleys, crestlines, and catchment basins. If we let water fall on this surface, it will concentrate over the minima of the surface. The surface drained by a minimum is called a *catchment basin*, and the common points between catchment basins are part of a network called the *watershed*.[9]

In practice, the algorithms do not work using this definition. Instead they use the notion of surface immersion. We can imagine the surface progressively immersed into water, in the same way as we threshold an image. Water will go up through the minima of the image, making ever-increasing lakes, which are labeled from the start. At a certain time, depending on the altitude of the points, lakes can merge. If we build dams to keep the lakes separated, and if we continue flooding the surface, we will end up with lakes separated by dams covering the surface. These dams are the watershed lines. Soille and Vincent[17] recently made an efficient implementation of the algorithm outlined here. The final segmentation using this algorithm results in compact regions separated by one-pixel-wide connected lines.

In our case, as we calculate the watershed on the complement of the filtered image, we find the valleys surrounding maxima, or summits, of the image. Both markers are united to form the complete marker image *Mf*:

$$Mf = Bm \cup Om \quad . \quad (5)$$

We show on Fig. 9 the shape and background markers superimposed on the original image.

3.3 Gradient Modification

Using the markers, we now eliminate the spurious edges in the gradient image. This is achieved again by morphological function reconstruction. This operation directly manipulates the gradient in such a way that only the strongest edge between the markers will generate a detectable contour for the final search algorithm. This time, instead of reconstructing the function using a marker under the function to be reconstructed, we use a marker that is over it, and work on the complement of the reconstructed function. By duality, instead of using dilation of the markers followed by intersection with the function to be reconstructed as in Eq. (3), we use erosion of the marker function, followed by union of the result with the function to be reconstructed. This dual-image reconstruction is implemented as follows.

drecons(*marker*,*constraint*) =

Repeat:

$$marker_{n+1} = \max[\varepsilon_B(marker_n), constraint]$$

until $marker_{n+1} = marker_n$, (6)

where $\varepsilon_B(marker)$ is the erosion of the marker function *marker* by the planar structuring element B.

Let G_{Mf} be the gray-level function originating from *Mf*:

$$G_{Mf} = -k_{Mf} + g_{max} \times (1 - k_{Mf}) \quad , \quad (7)$$

where g is the gradient image, g_{max} is the maximum value of the image g, and k_{Mf} is the indicator function of *Mf*. The filtered gradient image is then:

$$G_{final} = \text{drecons}(G_{Mf}, g) \quad . \quad (8)$$

Figure 6 illustrates how it works.

In the case of the maxima detector, the reconstruction has the effect of clipping peaks. In this case, it fills spurious minima and keeps only pertinent maxima of the function.

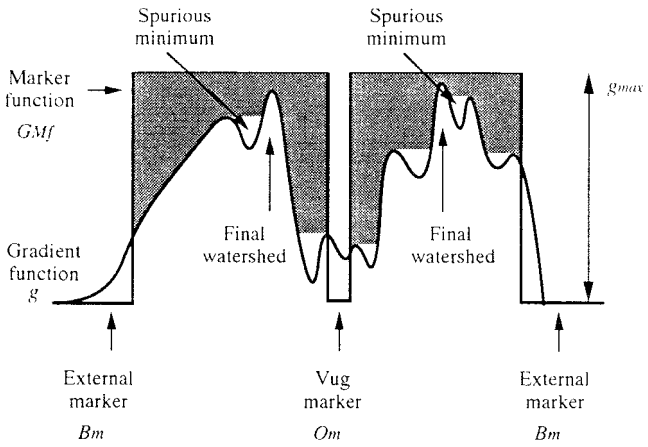

Fig. 6 The gradient modification is controlled by the marker function in order to suppress spurious minima leading to oversegmentation. Spurious minima are filled by the dual reconstruction of the marker function with the gradient function as the constraint function. The minima to be kept are specified by the markers.

3.4 *Contour Extraction*

With the gradient function morphologically reconstructed, the final contour extraction can now be performed. The watershed transformation has been proposed by Beucher and Lantuéjoul[9,18] to perform the task. The most similar approach to track contours on gradient images is from Martelli[7] who used a heuristic graph search on the image. The watershed transform has the advantage over the former of being nonparametric: There is no parameter to set and no heuristic to implement. Moreover, it is a global algorithm, intrinsically giving closed and thin contours:

$$contours = \text{watershed}(G_{final}) \tag{9}$$

4 Artifact Elimination

We experienced a problem while using the maxima detector to mark vugs: Homogeneous regions often exhibited smooth bumps that are not vugs. Because these bumps did not have as much contrast as real vugs, we thresholded markers against the image background. The problem is how to evaluate this background. Interpretation geologists have isolated a few criteria defining the background of the conductivity images. The background is associated with large plateaus, which are neither maxima nor minima. These plateaus vary smoothly. Generally, the background has a relatively low intensity.

From these criteria, we constructed a detection algorithm based on morphological filtering. First, we eliminate image minima smaller than a given size by using a closing ϕ: We perform a dilation on the image followed by a morphological dual reconstruction. Then, we eliminate maxima on the resulting image using an opening γ: We erode the image and then perform dual morphological reconstruction. The pixels of the image that have not changed are then considered to belong to the background. The structuring elements used are rectangles spanning the entire width of the image and 40 pixels deep. This is the default size that has been determined experimentally. The algorithm is robust with respect to this parameter. Figure 7 shows an example of background profile and how the detection algorithm works.

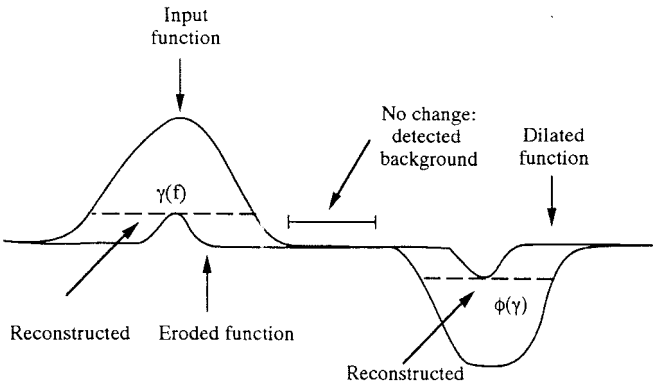

Fig. 7 Background detection by filtering. Plateaus larger than the size of the structuring element are unchanged and are regarded as background.

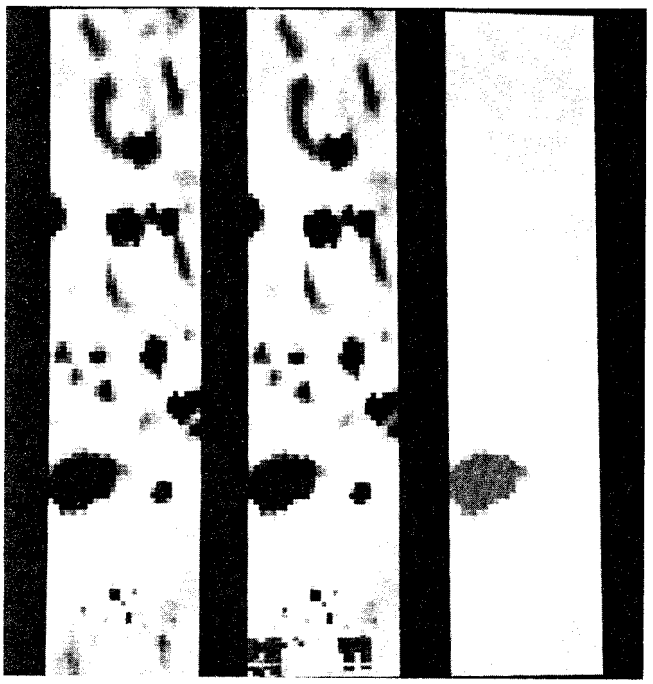

Fig. 8 Left: original image, middle: closing with reconstruction, right: opening with reconstruction. The closing eliminates minima smaller than the structuring element while the opening eliminates maxima. Note that, for illustration purposes, the size of the structuring element used in this example is 13×13 pixels instead of 40×27 pixels.

This gives us an adaptive threshold. This will not have any influence on the detection in the other zones delimited by the background marker. The filter equations are as follows:

$$\psi(f) = \gamma[\phi(f)] \ , \tag{10}$$

$$\gamma(f) = \text{recons}[\varepsilon_R(f), f] \ , \tag{11}$$

$$\phi(f) = \text{drecons}[\delta_R(f), f] \ , \tag{12}$$

where ψ is the morphological filter, f is the input image, *recons* and *drecons* are the morphological reconstruction operators, and R is the rectangular structuring element we used. Figure 8 shows the effects of openings and closings

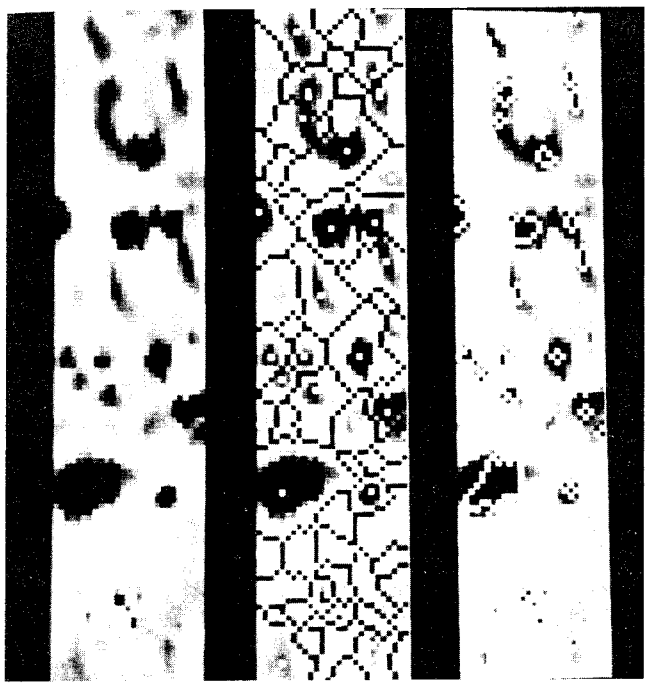

Fig. 9 Left: original image, center: vug (white dots) and background markers (dark mesh) over input image, right: contours found by the system (in white).

using reconstruction. The structuring elements used for the algorithm span all the height of the images shown in this paper. The structuring elements on these examples are squares having 13×13 pixels. We dramatically reduced the size of the structuring element for the purpose of illustration: The results would have been a uniform image at the size used for the application.

5 Experimental Results

We first tested the system on laboratory data obtained from a sandstone block into which holes of various diameters and depths had been drilled. Results strongly correlated with the actual diameters of the holes. In this paper, we present results obtained from real well data coming from carbonate reservoirs. Results correlated well with visual detection. Some differences observed were caused by incorrect artifact elimination. Some contours were slightly shifted compared to the contours found visually, but there were also differences when different geologists marked contours. There are two causes to these inconsistencies: The first one is a blurring effect caused by the point spread function of the acquisition system, which makes a visual ambiguity. The second cause is a visualization artifact: The dynamic range of the images is too wide for a CRT screen and this generates clipping effects, which may shift visual boundaries.

Figure 9 shows segmentation results. It seems at first sight that for some vugs the contours are overestimated or underestimated. This is caused by problems in the visualization as we mentioned earlier. We must also say a word on the precision on the measures. We detect small features in these images. Pixel size is large with respect to the size of most of the vugs. This is the cause of most of the imprecision of the measure. In digital images, a contour is not infinitely thin. It is composed of pixels having a measurable area. We must consider two possibilities when making measurements: The contour is inside or outside the vug. The difference between the measurement with and without the contour allows us to quantify the error caused by sampling effects.

The process of validation is still under way in order to compare the results obtained with information gathered from other sensors and core samples. This validation task is not easy: Problems accompany the comparison of results with actual cores because the electrical and optical images are dramatically different. We also have difficult problems in measuring the depth at which a sample and an image have been taken: Pixel size is in the millimeter scale while the measures of depth are 3 to 4 orders of magnitude larger. Nevertheless, we have encouraging results from the laboratory and from the field.

6 Discussion

The segmentation results are strongly dependent on the reliability of the markers. This segmentation strategy has the following advantages:

1. Fewer rules and parameters are needed compared to other techniques.
2. A marker is a binary set. It is less complex to process and manipulate than a full gray-level image or a set of filter parameters.
3. The approach is more related to the physical world. Marker parameters are usually more goal-oriented and physically justifiable than parameters such as thresholds or region-growing criteria.[1,2]
4. The marker generation modules, gradient operators, and edge detectors are all independent in the sense that algorithm changes to one module will not affect other modules in the processing chain. The well-admitted principle of modularity mentioned by Marr[3] is respected here. This gives to our strategy the flexibility segmentation systems badly need.
5. The user may even choose to place the markers on the image himself. Often, the tedious task for human operators is to measure objects. Recognition is generally not very difficult. Image processing algorithms usually have more problems recognizing objects than measuring them once they are recognized. We can take advantage of the strengths of both the operator and the system, letting the operator perform the recognition task and the algorithm perform the measurements and the fine segmentation.

This strategy is rather different from those generally proposed in the literature. Image understanding is carried out at the beginning using simple detectors. It is during this marker generation step that most of the "graceful degradation" is done. The aim of contour extraction is only to measure objects.

7 Conclusion

We presented an alternative approach to edge detection and region-growing segmentation. With the use of objects and background markers, it is possible to suppress spurious edges

by directly modifying gradient images before searching for the edges. The boundary is known to be located between the object and background marker surrounding it. The morphological function reconstruction acts as a spurious edge removal transformation. It leaves only the strongest gradient crest between edge and background markers. Afterward, any straightforward edge follower can be used in order to track the edge left by the reconstruction step. The watershed transformation by construction gives thin and closed contours, making it an excellent edge follower.

This segmentation strategy has the advantage of restricting the parameter setting process to the marker generation step. This makes the overall algorithm more robust and modular. It is then easier to validate, develop, and maintain.

References

1. S. W. Zucker, "Region growing: childhood and adolescence," *Comput. Vision Graphics Image Proc.* **5,** 382–399 (1976).
2. A. Gagalowicz and O. Monga, "A new approach for image segmentation," *Proc. IAPR 8th Int. Conf. Pattern Recognition,* Paris, pp. 265–267 (1986).
3. D. Marr, "Early processing of visual information," *Phil. Trans. Royal Soc. London* **B.275,** 483–524 (1976).
4. D. Marr and E. Hildreth, "Theory of edge detection," *Proc. Royal Soc. London* **B207,** 187–217 (1980).
5. I. E. Abdou and W. K. Pratt, "Quantitative design and evaluation of enhancement/thresholding edge detectors," *Proc. IEEE* **67**(5), 753–763 (1979).
6. J. Lester, H. Williams, B. Weintraub, and J. Brenner, "Two graph searching techniques for boundary finding in white blood cell images," *Comput. Bio. Med.* **8,** 293–308 (1978).
7. A. Martelli, "Edge detection using heuristic search methods," *Comput. Vision, Graphics, Image Proc.* **1,** 335–345 (1971).
8. E. De Micheli, B. Caprile, P. Ottonello, and V. Torre, "Localization and noise in edge detection," *IEEE Trans. Pattern Analysis Machine Intell.* **PAMI-11**(10), 1106–1116 (1989).
9. S. Beucher and C. Lantuéjoul, "Use of watersheds in contour detection," *IRISA Int. Workshop Image Processing: Real-Time Edge and Motion Detection/Estimation,* 2.1–2.12 (1979).
10. Serge Beucher, "Segmentation d'images et morphologie mathématique," PhD thesis, Ecole des Mines de Paris (1990).
11. F. Meyer and S. Beucher, "Morphological segmentation," *J. Visual Comm. Image Representation* **1**(1), 21–46 (Sep. 1990).
12. Serge Beucher, "Lecture automatique des gels d'électrophorèse," Technical Report N-746, Centre de Géostatistique et Morphologie Mathématique, Ecole des Mines de Paris (1982).
13. S. Beucher, M. Bilodeau, and X. Yu, "Road segmentation by watershed algorithms," *INRIA Prometheus Workshop,* 8–31 (1990).
14. F. Friedlander, "Le traitement morphologique d'images de cardiologie nucléaire," PhD thesis, Ecole des Mines de Paris (1989).
15. M. P. Ekstrom, C. Dahan, M.-Y. Chen, P. Loyd, and D. Rossi, "Formation imaging with microelectrical scanning arrays," *The Log Analyst* **28**(3), 294–306 (1987).
16. P. Soille and M. M. Ansoult, "Automated basin delineation from digital elevation models using mathematical morphology," *Signal Proc.* **20,** 171–182 (1990).
17. P. Soille and L. Vincent, "Determining watersheds in digital pictures via flooding simulations," *Proc. SPIE* **1360,** 240–250 (1990).
18. S. Beucher, "Watersheds of functions and picture segmentation," *ICASSP 82, Proc. IEEE Int. Conf. Acoustics, Speech and Signal Processing,* pp. 1928–1931 (1982).

Jean-Francois Rivest received his BSc in engineering physics from Université Laval, Québec, Canada, in 1986, his MSc in biomedical engineering from Ecole Polytechnique de Montréal, Canada, in 1988, and a Diplôme d'Etudes Approfondies in artificial intelligence, pattern recognition, and computer graphics from Université Pierre et Marie Curie (Paris VI) in 1989. Currently, he is a PhD candidate in the Centre de Morphologie Mathématique, Ecole des Mines de Paris. His current interests are in imaging applications to oil well technology, image segmentation, and engineering aspects of image analysis. He is a member of IEEE, IEEE Computer Society, SPIE, and Ordre des Ingénieurs de Québec.

Serge Beucher received his engineering degree from the Institut National Polytechnique de Lorraine in 1975. In 1977, he joined the Centre de Morphologie Mathématique (CMM) of the Ecole des Mines de Paris at Fontainebleau, where he was involved in many projects in image analysis and hardware design. He received his PhD in mathematical morphology from the Ecole des Mines in 1990. Since 1986, he has been in charge of the industrial vision team at CMM. His research activities include applications and developments in mathematical morphology, image segmentation, scene analysis, and process control. He is a member of the International Society of Stereology.

Jean-Pierre Delhomme is a technical consultant at Etudes et Productions Schlumberger in Clamart, France. His current interests include applications of borehole imaging to the characterization of hydrocarbon reservoirs. He holds an engineering degree from Ecole Centrale de Paris. He received his doctorate degree in geostatistics from Ecole des Mines de Paris where he was a research associate until he joined Schlumberger in 1980.